

Search for the Decays $B_d^0 \rightarrow \gamma\gamma$ and $B_s^0 \rightarrow \gamma\gamma$

The L3 Collaboration

Abstract

A search for the decays $B_{d,s}^0 \rightarrow \gamma\gamma$ in 2.95 million hadronic Z decays has been performed using the L3 detector at LEP. No candidates are found in the signal region and upper limits have been set on the branching ratios: $\text{Br}(B_d^0 \rightarrow \gamma\gamma) < 3.9 \times 10^{-5}$ and $\text{Br}(B_s^0 \rightarrow \gamma\gamma) < 14.8 \times 10^{-5}$ at 90% CL. These are the first limits set on these exclusive rare decays.

(Submitted to *Physics Letters B*)

Introduction

Measurements of rare B hadron decays are important discriminators to test the Standard Model (SM) as well as to probe the physics beyond it. Of particular interest are the decays $B_{d,s}^0 \rightarrow \gamma\gamma$ for which there has been no experimental measurement until now. The decays correspond to a second order weak transition, including gluonic penguins, followed by annihilation, often referred to as an “effective” flavor-changing weak neutral current process, as shown by some diagrams in Figure 1. The expected branching ratio for this decay mode is $\sim 10^{-7}$ in the SM, although there are large theoretical uncertainties [1–4]. As pointed out by Falk [5] exclusive decay rates are extremely difficult to compute reliably. Observation of these decays could lead to a direct measurement of the Cabibbo-Kobayashi-Maskawa (CKM) matrix elements $|V_{ts}|$ and $|V_{td}|$. In contrast to the theoretical situation, experimentally $B^0 \rightarrow \gamma\gamma$ is a relatively clean channel to study.

It is believed that for some non-standard scenarios, such as two-Higgs-doublets and minimal supersymmetric models, the $B^0 \rightarrow \gamma\gamma$ decay rate can be significantly enhanced [1]. Thus any observation of the decay $B^0 \rightarrow \gamma\gamma$ at an unusual rate could be an indication of new physics.

This analysis exploits the high resolution BGO electromagnetic calorimeter of the L3 detector which is well suited for this purpose. The analysis is performed on data recorded in 1991 through 1994 at $\sqrt{s} \approx M_Z$, corresponding to a sample of 2.95 million $e^+e^- \rightarrow \text{hadron}$ events. The mixed sample of B hadrons available in Z decays provides an opportunity to study B_s^0 meson decays which are not accessible at the center-of-mass energy of the $\Upsilon(4S)$.

The L3 Detector

The L3 detector is described in detail in reference 6. It consists of a central tracking chamber, a high resolution electromagnetic calorimeter composed of bismuth germanium oxide (BGO) crystals, a ring of plastic scintillation counters, a uranium and brass hadron calorimeter with proportional wire chamber readout, and an accurate muon chamber system. These detectors are installed in a 12 m diameter magnet which provides a uniform field of 0.5 T along the beam direction.

The central tracking chamber is a time expansion chamber (TEC) with high spatial resolution in the r - ϕ plane normal to the beam. A chamber mounted just outside the TEC provides z-coordinate measurements.

The material preceding the barrel part of the electromagnetic calorimeter amounts to less than 10% of a radiation length. In this region the energy resolution of the BGO calorimeter is better than 2% for energies above 1 GeV. The angular resolution of electromagnetic clusters is better than 0.5° for energies above 1 GeV.

Event Selection

Hadronic events selected with a standard set of cuts [7] are used for this analysis. Candidate photons in an event are selected in the barrel electromagnetic calorimeter with $|\cos \theta| \leq 0.75$, where θ is the polar angle, and are recognized as isolated energy clusters in the electromagnetic calorimeter with a shower shape consistent with that of electromagnetic particles. To ensure

that the electromagnetic cluster corresponds to a photon, there should be no charged track within 10 mrad of the electromagnetic cluster in the plane transverse to the beam direction.

We use JETSET [8] simulated b-flavor events, requiring the decay chain $B_{d,s}^0 \rightarrow \gamma\gamma$, for one of the $B_{d,s}^0$ mesons. The mass of the B_d^0 and B_s^0 generated in the Monte Carlo are 5279 MeV and 5373 MeV respectively. The modified Peterson fragmentation function [9] is used as a function of $x_E = 2E_{hadron}/\sqrt{s}$ with the parameter $\epsilon_b = 0.05$. For the background studies a sample of approximately 2.1 million hadronic Z events were generated and simulated using the JETSET Monte Carlo program.

Due to the hard fragmentation of the b quark, the energy carried by the two photons from a B^0 decay is large. The sum of the two photon energies is required to be more than 25 GeV as shown in Figure 2a, where the combinatorial background is peaked at small energies in contrast to the $B^0 \rightarrow \gamma\gamma$ Monte Carlo events. In addition it is required that the opening angle between the two photons $\theta_{\gamma\gamma}$ be less than 40° as shown in Figure 2b. In this case the combinatorial background tends to be at large angles. These cuts reduce the combinatorial background either from the low energy photons or from the opposite hemisphere. The invariant mass of the $\gamma\gamma$ system is reconstructed with photons having a minimum energy of 2 GeV.

In order to separate $b\bar{b}$ events from other hadronic events, a multidimensional analysis based on a neural network approach described elsewhere [7] is used. It has been verified that the neural network response for $B_{d,s}^0 \rightarrow \gamma\gamma$ has the same shape as for other $b\bar{b}$ events. The efficiency calculation is based on a full simulation of the L3 detector [10] allowing for the effects of energy loss, multiple scattering, interactions and decays in the detector material as well as time-dependent detector effects.

Figure 3(a,b) shows the $\gamma\gamma$ invariant mass of the $B_{d,s}^0$ Monte Carlo events. A Gaussian fit is performed on the invariant mass distributions for B_d^0 and B_s^0 separately. The mass resolutions obtained are $\sigma = 72$ MeV, which is to be compared with the mass difference $M_{B_s^0} - M_{B_d^0} = 94$ MeV. The efficiency for this process within the 2σ mass window of the $B_{d,s}^0$ is calculated to be $0.227 \pm 0.007 \pm 0.006$ using all preselected events and $0.118 \pm 0.005 \pm 0.007$ with the additional $b\bar{b}$ selection requirement based on the neural network, where the first error is statistical and the second is systematic. The systematic uncertainties are evaluated by varying the selection criteria and the fragmentation function as shown in Table 1.

Source	$\Delta \epsilon_{B^0 \rightarrow \gamma\gamma}$
Electromagnetic Shower Shape	± 0.0033
Track Veto	± 0.0028
Opening Angle $\theta_{\gamma\gamma}$	± 0.0005
Energy sum of the two photons	± 0.0018
$b\bar{b}$ Selection	± 0.0035
Fragmentation	± 0.0036
Total	± 0.0069

Table 1: Systematic uncertainties on the efficiency for $B^0 \rightarrow \gamma\gamma$ Monte Carlo events.

A $B^0 \rightarrow \pi^0\pi^0$ decay can fake a $B^0 \rightarrow \gamma\gamma$ decay, if π^0 's are very energetic such that the two photons from π^0 decay merge into single cluster. We make the conservative assumption that the contribution $B^0 \rightarrow \pi^0\pi^0$ is negligible. Searches for $B^0 \rightarrow \pi^0\pi^0/\pi^0\eta/\eta\eta$ are described in reference 11.

Results

Figure 3(c,d) shows the invariant mass distribution of the $\gamma\gamma$ system for all events and for the $b\bar{b}$ enriched sample in data and five-flavor $Z \rightarrow q\bar{q}$ Monte Carlo events. As one can see from Figure 3c the shape of the background is well reproduced by the five-flavor $q\bar{q}$ Monte Carlo events. With the additional $b\bar{b}$ selection requirement based on the neural network, no candidates are observed within $\pm 2\sigma$ mass window of $B_{d,s}^0$ (see Figure 3d).

Upper limits on the exclusive branching ratio for the B_d^0 and B_s^0 mesons decaying into two photons are obtained using a binned likelihood fit to the $\gamma\gamma$ invariant mass distribution. The background is estimated from the shape of the invariant mass distribution in the data shown in Figure 3d. An exponential function is fitted to the invariant mass distribution in the range 4.4 GeV to 6.0 GeV, excluding the $B_{d,s}^0$ mass window. For the signal there are two components, corresponding to B_d^0 and B_s^0 . The overlapping region of B_d^0 and B_s^0 is taken into account using the Monte Carlo $\gamma\gamma$ mass distributions. The total likelihood function is given by:

$$\mathcal{L}(\mu_d, \mu_s) = \prod_{i=1}^n \frac{e^{-(\mu_{b,i} + \mu_{d,i} + \mu_{s,i})} (\mu_{b,i} + \mu_{d,i} + \mu_{s,i})^{N_i}}{N_i!}$$

where i is the bin number; N_i are the number of observed events in bin i ; μ_b is the background component and μ_d, μ_s are the B_d^0 and B_s^0 signal components respectively. The total signal components are given by:

$$\mu_q = \sum_i \mu_{q,i} = \text{Br}(B_q^0 \rightarrow \gamma\gamma) \times N_h \times 2 \times R_{b\bar{b}} \times f_{b \rightarrow q} \times \epsilon_{B_q^0 \rightarrow \gamma\gamma} \quad (\text{for } q = d, s)$$

where N_h is the total number of hadronic Z decays, $R_{b\bar{b}}$ is taken from the L3 measurement [7], and $f_{b \rightarrow d,s}$ is the fraction of $b \rightarrow B_d^0 = 39.5 \pm 4.0\%$ and $b \rightarrow B_s^0 = 12.0 \pm 3.0\%$ used, in agreement with the available measurements [12], while $\epsilon_{B_q^0 \rightarrow \gamma\gamma}$ denotes the selection efficiency for $B_{d,s}^0 \rightarrow \gamma\gamma$.

The likelihood is evaluated as a function of the branching ratios $\text{Br}(B_d^0 \rightarrow \gamma\gamma)$ and $\text{Br}(B_s^0 \rightarrow \gamma\gamma)$, taking into account errors on the efficiency, $R_{b\bar{b}}$, $f_{b \rightarrow d,s}$ and the background parameterization. By varying $\text{Br}(B_d^0 \rightarrow \gamma\gamma)$ and $\text{Br}(B_s^0 \rightarrow \gamma\gamma)$ simultaneously we obtain the two dimensional likelihood distribution for different confidence levels. The one dimensional 90% confidence level upper limits on the B_d^0 (B_s^0) branching ratios are obtained by integrating the likelihood over all the values of the B_s^0 (B_d^0) branching ratios. The 90% confidence level limits obtained are

$$\text{Br}(B_d^0 \rightarrow \gamma\gamma) < 3.9 \times 10^{-5} \quad \text{at } 90\% \text{ CL,}$$

$$\text{Br}(B_s^0 \rightarrow \gamma\gamma) < 14.8 \times 10^{-5} \quad \text{at } 90\% \text{ CL.}$$

A complementary analysis not relying on the neural network $b\bar{b}$ selection has been performed as a cross-check. This analysis uses photon selection and global kinematic variables similar to

those used in reference 11. A single variable function based on a multidimensional approach has been used to discriminate the signal from the background events. This gives compatible results with the analysis described in this paper.

Conclusion

A search for the exclusive rare decays $B_{d,s}^0 \rightarrow \gamma\gamma$ in 2.95 million hadronic Z decays has been performed. No candidates are observed in the data within the mass window of $B_{d,s}^0$. Upper limits on these decay modes have been set:

$$\text{Br}(B_d^0 \rightarrow \gamma\gamma) < 3.9 \times 10^{-5} \quad \text{at 90\% CL,}$$

$$\text{Br}(B_s^0 \rightarrow \gamma\gamma) < 14.8 \times 10^{-5} \quad \text{at 90\% CL.}$$

The present results are the first limits set on the above branching ratios.

Acknowledgments

We wish to express our gratitude to the CERN accelerator divisions for the excellent performance of the LEP machine. We acknowledge with appreciation the effort of all engineers, technicians and support staff who have participated in the construction and maintenance of this experiment. Those of us who are not from member states thank CERN for its hospitality and help.

References

- [1] G. Lin *et al.*, Phys. Rev. **D 42** (1990) 2314.
- [2] S. Herrlich and J. Kalinowski, Nucl. Phys. **B 381** (1992) 501.
- [3] J. O. Eeg and I. Picek, Phys. Lett. **B 336** (1994) 549.
- [4] J. Trampetic, FIZIKA **B 2** (1993) 121.
- [5] A. F. Falk, Review Talk on Theory of Rare B decays, International Symposium on Vector Boson Self-Interactions, University of California, Los Angeles, February 1-3, 1995. Preprint: JHU-TIPAC-950006.
- [6] L3 Collaboration, B. Adeva *et al.*, Nucl. Instr. Meth. **A 289** (1990) 35;
L3 Collaboration, O. Adriani *et al.*, Phys. Rep. **236** (1993) 1.
- [7] L3 Collaboration, O. Adriani *et al.*, Phys. Lett. **B 307** (1993) 237.
- [8] T. Sjöstrand and M. Bengtsson, Comput. Phys. Commun. **43** (1987) 367;
"PYTHIA 5.6 and JETSET 7.3: Physics and manual", preprint CERN-TH.6488/92.
- [9] C. Peterson *et al.*, Phys. Rev. **D 27** (1983) 105.
- [10] The L3 detector simulation is based on GEANT Version 3.15. See R. Brun *et al.*, "GEANT 3", CERN DD/EE/84-1 (Revised), September 1987. The GHEISHA program (H. Fesefeldt, RWTH Aachen Report PITHA 85/02 (1985)) is used to simulate hadronic interactions.
- [11] L3 Collaboration, M. Acciarri *et al.* Search for Neutral Charmless B Decays at LEP , Preprint CERN-PPE/95-124, Submitted to Phys. Lett. **B**.
- [12] OPAL Collaboration, R. Akers *et al.*, Z. Phys. **C 66** (1995) 555;
OPAL Collaboration, R. Akers *et al.*, Z. Phys. **C 67** (1995) 57;
ALEPH Collaboration, D. Buskulic *et al.*, Preprint CERN-PPE/95-092, Submitted to Z. Phys. **C**;
ALEPH Collaboration, D. Buskulic *et al.*, Preprint CERN-PPE/95-094, Submitted to Phys. Lett. **B**.

The L3 Collaboration:

M. Acciarri,²⁷ A. Adam,⁴⁶ O. Adriani,¹⁷ M. Aguilar-Benitez,²⁶ S. Ahlen,¹¹ B. Alpat,³⁴ J. Alcaraz,²⁶ J. Allaby,¹⁸ A. Aloisio,²⁹ G. Alverson,¹² M. G. Alvigi,²⁹ G. Ambrosi,³⁴ H. Anderhub,⁴⁹ V. P. Andreev,³⁸ T. Angelescu,¹³ D. Antreasyan,⁹ A. Arefev,²⁸ T. Azemoon,³ T. Aziz,¹⁰ P. Bagnaia,^{37,18} L. Baksay,⁴⁴ R. C. Ball,³ S. Banerjee,¹⁰ K. Banicz,⁴⁶ R. Barillere,¹⁸ L. Barone,³⁷ P. Bartalini,³⁴ A. Baschirotto,²⁷ M. Basile,⁹ R. Battiston,³⁴ A. Bay,²³ F. Becattini,¹⁷ U. Becker,¹⁶ F. Behner,⁴⁹ Gy. L. Bencze,¹⁴ J. Berdugo,²⁶ P. Berges,¹⁶ B. Bertucci,¹⁸ B. L. Betev,⁴⁹ M. Biasini,³⁴ A. Biland,⁴⁹ G. M. Bilei,³⁴ R. Bizzarri,³⁷ J. J. Blaising,¹⁸ G. J. Bobbink,² R. Bock,¹ A. Böhm,¹ B. Borgia,³⁷ A. Boucham,⁴ D. Bourilkov,⁴⁹ M. Bourquin,²⁰ D. Boutigny,⁴ E. Brambilla,¹⁶ J. G. Branson,⁴⁰ V. Brigljevic,⁴⁹ I. C. Brock,³⁵ A. Buijs,⁴⁵ A. Bujak,⁴⁶ J. D. Burger,¹⁶ W. J. Burger,²⁰ C. Burgos,²⁶ J. Busenitz,⁴⁴ A. Buytenhuijs,³¹ X. D. Cai,¹⁹ M. Capell,¹⁶ G. Cara Romeo,⁹ M. Caria,³⁴ G. Carlino,²⁹ A. M. Cartacci,¹⁷ J. Casaus,²⁶ G. Castellini,¹⁷ R. Castello,²⁷ F. Cavallari,³⁷ N. Cavallo,²⁹ C. Cecchi,²⁰ M. Cerrada,²⁶ F. Cesaroni,³⁷ M. Chamizo,²⁶ A. Chan,⁵¹ Y. H. Chang,⁵¹ U. K. Chaturvedi,¹⁹ M. Chemarin,²⁵ A. Chen,⁵¹ C. Chen,⁷ G. Chen,⁷ G. M. Chen,⁷ H. F. Chen,²¹ H. S. Chen,⁷ M. Chen,¹⁶ G. Chiefari,²⁹ C. Y. Chien,⁵ M. T. Choi,⁴³ L. Cifarelli,³⁹ F. Cindolo,⁹ C. Civinini,¹⁷ I. Clare,¹⁶ R. Clare,¹⁶ T. E. Coan,²⁴ H. O. Cohn,³² G. Coignet,⁴ A. P. Colijn,² N. Colino,¹⁸ V. Commichau,¹ S. Costantini,³⁷ F. Cotorobai,¹³ B. de la Cruz,²⁶ T. S. Dai,¹⁶ R. D' Alessandro,¹⁷ R. de Asmundis,²⁹ H. De Boeck,³¹ A. Degré,⁴ K. Deiters,⁴⁷ E. Dénes,¹⁴ P. Denes,³⁶ F. DeNotaristefani,³⁷ D. DiBitonto,⁴⁴ M. Diemoz,³⁷ D. van Dierendonck,² F. Di Lodovico,³⁷ C. Dionisi,³⁷ M. Dittmar,⁴⁹ A. Dominguez,⁴⁰ A. Doria,²⁹ I. Dorne,⁴ M. T. Dova,^{19,8} E. Drago,²⁹ D. Duchesneau,¹⁸ P. Duinker,² I. Duran,⁴¹ S. Dutta,¹⁰ S. Easo,³⁴ Yu. Efremenko,³² H. El Mamouni,²⁵ A. Engler,³⁵ F. J. Eppling,¹⁶ F. C. Erné,² J. P. Ernenwein,²⁵ P. Extermann,²⁰ R. Fabbretti,⁴⁷ M. Fabre,³⁷ R. Faccini,³⁷ S. Falciano,³⁷ A. Favara,¹⁷ J. Fay,²⁵ M. Felcini,⁴⁹ T. Ferguson,³⁵ D. Fernandez,²⁶ G. Fernandez,²⁶ F. Ferroni,³⁷ H. Fesefeldt,¹ E. Fiandrin,³⁴ J. H. Field,²⁰ F. Filthaut,³⁵ P. H. Fisher,¹⁶ G. Forconi,¹⁶ L. Fredj,²⁰ K. Freudenreich,⁴⁹ M. Gailoud,²³ Yu. Galaktionov,^{28,16} S. N. Ganguli,¹⁰ P. Garcia-Abia,²⁶ S. S. Gau,¹² S. Gentile,³⁷ J. Gerald,⁵ N. Gheordanescu,¹³ S. Giagu,³⁷ S. Goldfarb,²³ J. Goldstein,¹¹ Z. F. Gong,²¹ E. Gonzalez,²⁶ A. Gougas,⁵ D. Goujon,²⁰ G. Gratta,³³ M. W. Gruenewald,⁸ V. K. Gupta,³⁶ A. Gurtu,¹⁰ H. R. Gustafson,³ L. J. Gutay,⁴⁶ B. Hartmann,¹ A. Hasan,³⁰ J. T. He,⁷ T. Hebbeker,⁸ A. Hervé,¹⁸ K. Hilgers,¹ W. C. van Hoek,³¹ H. Hofer,⁴⁹ H. Hoorani,²⁰ S. R. Hou,⁵¹ G. Hu,¹⁹ M. M. Ilyas,¹⁹ V. Innocent,¹⁸ H. Janssen,⁴ B. N. Jin,⁷ L. W. Jones,³ P. de Jong,¹⁶ I. Josa-Mutuberria,²⁶ A. Kasser,²³ R. A. Khan,¹⁹ Yu. Kamyshev,³² P. Kapinos,⁴⁸ J. S. Kapustinsky,²⁴ Y. Karyotakis,⁴ M. Kaur,^{19,◇} M. N. Kienzle-Focacci,²⁰ D. Kim,⁵ J. K. Kim,⁴³ S. C. Kim,⁴³ Y. G. Kim,⁴³ W. W. Kinnison,²⁴ A. Kirkby,³³ D. Kirkby,³³ J. Kirkby,¹⁸ W. Kittel,³¹ A. Klimentov,^{16,28} A. C. König,³¹ E. Koffeman,¹ O. Kornadt,¹ V. Koutsenko,^{16,28} A. Koulbardi,³⁸ R. W. Kraemer,³⁵ T. Kramer,¹⁶ W. Krenz,¹ H. Kuijten,³¹ A. Kunin,^{16,28} P. Ladron de Guevara,²⁶ G. Landi,¹⁷ C. Lapoint,¹⁶ K. Lassila-Perini,⁴⁹ P. Laurikainen,²² M. Lebeau,¹⁸ A. Lebedev,¹⁶ P. Lebrun,²⁵ P. Lecomte,⁴⁹ P. Lecoq,¹⁸ P. Le Coultre,⁴⁹ J. S. Lee,⁴³ K. Y. Lee,⁴³ C. Leggett,³ J. M. Le Goff,⁸ R. Leiste,⁴⁸ M. Lenti,¹⁷ E. Leonardi,³⁷ P. Levchenko,³⁸ C. Li,²¹ E. Lieb,⁴⁸ W. T. Lin,⁵¹ F. L. Linde,² B. Lindemann,¹ L. Lista,²⁹ Z. A. Liu,⁷ W. Lohmann,⁴⁸ E. Longo,³⁷ W. Lu,³³ Y. S. Lu,⁷ K. Lübelmeyer,¹ C. Luci,³⁷ D. Luckey,¹⁶ L. Ludovici,³⁷ L. Luminari,³⁷ W. Lustermann,⁴⁷ W. G. Ma,²¹ A. Macchiolo,¹⁷ M. Maity,¹⁰ L. Malgeri,³⁷ A. Malinin,²⁸ C. Maña,²⁶ S. Mangla,¹⁰ M. Maolinbay,⁴⁹ P. Marchesini,⁴⁹ A. Marin,¹¹ J. P. Martin,²⁵ F. Marzano,³⁷ G. G. G. Massaro,² K. Mazumdar,¹⁰ D. McNally,¹⁸ S. Mele,²⁹ L. Merola,²⁹ M. Meschini,¹⁷ W. J. Metzger,³¹ Y. Mi,²³ A. Mihul,¹³ A. J. W. van Mil,³¹ G. Mirabelli,³⁷ J. Mnich,¹⁸ M. Möller,¹ B. Monteleoni,¹⁷ R. Moore,³ R. Morand,⁴ S. Morganti,³⁷ R. Mount,³³ S. Müller,¹ F. Muheim,²⁰ E. Nagy,¹⁴ S. Nahn,¹⁶ M. Napolitano,²⁹ F. Nessi-Tedaldi,⁴⁹ H. Newman,³³ A. Nippe,¹ H. Nowak,⁴⁸ G. Organtini,³⁷ R. Ostonen,²² D. Pandoulas,¹ S. Paoletti,³⁷ P. Paolucci,²⁹ G. Pascale,³⁷ G. Passaleva,¹⁷ S. Patricelli,²⁹ T. Paul,³⁴ M. Pauluzzi,³⁴ C. Paus,¹ F. Pauss,⁴⁹ Y. J. Pei,¹ S. Pensotti,²⁷ D. Perret-Gallix,⁴ S. Petrak,⁸ A. Pevsner,⁵ D. Piccolo,²⁹ M. Pieri,¹⁷ J. C. Pinto,³⁵ P. A. Piroué,³⁶ E. Pistolesi,¹⁷ V. Plyaskin,²⁸ M. Pohl,⁴⁹ V. Pojidaev,^{28,17} H. Postema,¹⁶ N. Produit,²⁰ R. Raghavan,¹⁰ G. Rahal-Callot,⁴⁹ P. G. Rancoita,²⁷ M. Rattaggi,²⁷ G. Raven,⁴⁰ P. Razi,³⁰ K. Read,³² M. Redaelli,²⁷ D. Ren,⁴⁹ M. Rescigno,³⁷ S. Reucroft,¹² A. Ricker,¹ S. Riemann,⁴⁸ B. C. Riemers,⁴⁶ K. Riles,³ O. Rind,³ S. Ro,⁴³ A. Robohm,⁴⁹ J. Rodin,¹⁶ F. J. Rodriguez,²⁶ B. P. Roe,³ M. Röhner,¹ S. Röhner,¹ L. Romero,²⁶ S. Rosier-Lees,⁴ Ph. Rosset,²³ W. van Rossum,⁴⁵ S. Roth,¹ J. A. Rubio,¹⁸ H. Rykaczewski,⁴⁹ J. Salicio,¹⁸ J. M. Salicio,²⁶ E. Sanchez,²⁶ A. Santocchia,³⁴ M. E. Sarakinos,²² S. Sarkar,¹⁰ M. Sassowsky,¹ G. Sauvage,⁴ C. Schäfer,¹ V. Schegelsky,³⁸ D. Schmitz,¹ P. Schmitz,¹ M. Schneegans,⁴ B. Schoeneich,⁴⁸ N. Scholz,⁴⁹ H. Schopper,⁵⁰ D. J. Schotanus,³¹ R. Schulte,¹ K. Schultze,¹ J. Schwenke,¹ G. Schwering,¹ C. Sciacca,²⁹ P. G. Seiler,⁴⁷ J. C. Sens,⁵¹ L. Servoli,³⁴ S. Shevchenko,³³ N. Shivarov,⁴² V. Shoutko,²⁸ J. Shukla,²⁴ E. Shumilov,²⁸ D. Son,⁴³ A. Sopczak,¹⁸ V. Soulimov,²⁹ B. Smith,¹⁶ T. Spickermann,¹ P. Spillantini,¹⁷ M. Steuer,¹⁶ D. P. Stickland,³⁶ F. Sticozzi,¹⁶ H. Stone,³⁶ B. Stoyanov,⁴² K. Strauch,¹⁵ K. Sudhakar,¹⁰ G. Sultanov,¹⁹ L. Z. Sun,²¹ G. F. Susinno,²⁰ H. Suter,⁴⁹ J. D. Swain,¹⁹ X. W. Tang,⁷ L. Tauscher,⁶ L. Taylor,¹² Samuel C. C. Ting,¹⁶ S. M. Ting,¹⁶ O. Toker,³⁴ F. Tonisch,⁴⁸ M. Tonutti,¹ S. C. Tonwar,¹⁰ J. Tóth,¹⁴ A. Tsaregorodtsev,³⁸ G. Tsipolitis,³⁵ C. Tully,³⁶ H. Tuchscherer,⁴⁴ J. Ulbricht,⁴⁹ L. Urbán,¹⁴ U. Uwer,¹ E. Valente,³⁷ R. T. Van de Walle,³¹ I. Vetlitsky,²⁸ G. Viertel,⁴⁹ M. Vivargent,⁴ R. Völkert,⁴⁸ H. Vogel,³⁵ H. Vogt,⁴⁸ I. Vorobiev,²⁸ A. A. Vorobyov,³⁸ An. A. Vorobyov,³⁸ L. Vuilleumier,²³ M. Wadhwa,⁶ W. Wallraff,¹ J. C. Wang,¹⁶ X. L. Wang,²¹ Y. F. Wang,¹⁶ Z. M. Wang,²¹ A. Weber,¹ R. Weill,²³ C. Willmott,²⁶ F. Wittgenstein,¹⁸ S. X. Wu,¹⁹ S. Wynhoff,¹ J. Xu,¹¹ Z. Z. Xu,²¹ B. Z. Yang,²¹ C. G. Yang,⁷ X. Y. Yao,⁷ J. B. Ye,²¹ S. C. Yeh,⁵¹ J. M. You,³⁵ C. Zaccardelli,³³ An. Zalite,³⁸ P. Zemp,⁴⁹ J. Y. Zeng,⁷ Y. Zeng,¹ Z. Zhang,⁷ Z. P. Zhang,²¹ B. Zhou,¹¹ G. J. Zhou,⁷ J. F. Zhou,¹ Y. Zhou,³ G. Y. Zhu,⁷ R. Y. Zhu,³³ A. Zichichi,^{9,18,19} B. C. C. van der Zwaan.²

-
- 1 I. Physikalisches Institut, RWTH, D-52056 Aachen, FRG[§]
 - III. Physikalisches Institut, RWTH, D-52056 Aachen, FRG[§]
 - 2 National Institute for High Energy Physics, NIKHEF, and University of Amsterdam, NL-1009 DB Amsterdam, The Netherlands
 - 3 University of Michigan, Ann Arbor, MI 48109, USA
 - 4 Laboratoire d'Annecy-le-Vieux de Physique des Particules, LAPP, IN2P3-CNRS, BP 110, F-74941 Annecy-le-Vieux CEDEX, France
 - 5 Johns Hopkins University, Baltimore, MD 21218, USA
 - 6 Institute of Physics, University of Basel, CH-4056 Basel, Switzerland
 - 7 Institute of High Energy Physics, IHEP, 100039 Beijing, China
 - 8 Humboldt University, D-10099 Berlin, FRG[§]
 - 9 INFN-Sezione di Bologna, I-40126 Bologna, Italy
 - 10 Tata Institute of Fundamental Research, Bombay 400 005, India
 - 11 Boston University, Boston, MA 02215, USA
 - 12 Northeastern University, Boston, MA 02115, USA
 - 13 Institute of Atomic Physics and University of Bucharest, R-76900 Bucharest, Romania
 - 14 Central Research Institute for Physics of the Hungarian Academy of Sciences, H-1525 Budapest 114, Hungary[‡]
 - 15 Harvard University, Cambridge, MA 02139, USA
 - 16 Massachusetts Institute of Technology, Cambridge, MA 02139, USA
 - 17 INFN Sezione di Firenze and University of Florence, I-50125 Florence, Italy
 - 18 European Laboratory for Particle Physics, CERN, CH-1211 Geneva 23, Switzerland
 - 19 World Laboratory, FBLJA Project, CH-1211 Geneva 23, Switzerland
 - 20 University of Geneva, CH-1211 Geneva 4, Switzerland
 - 21 Chinese University of Science and Technology, USTC, Hefei, Anhui 230 029, China
 - 22 SEFT, Research Institute for High Energy Physics, P.O. Box 9, SF-00014 Helsinki, Finland
 - 23 University of Lausanne, CH-1015 Lausanne, Switzerland
 - 24 Los Alamos National Laboratory, Los Alamos, NM 87544, USA
 - 25 Institut de Physique Nucléaire de Lyon, IN2P3-CNRS, Université Claude Bernard, F-69622 Villeurbanne Cedex, France
 - 26 Centro de Investigaciones Energeticas, Medioambientales y Tecnológicas, CIEMAT, E-28040 Madrid, Spain
 - 27 INFN-Sezione di Milano, I-20133 Milan, Italy
 - 28 Institute of Theoretical and Experimental Physics, ITEP, Moscow, Russia
 - 29 INFN-Sezione di Napoli and University of Naples, I-80125 Naples, Italy
 - 30 Department of Natural Sciences, University of Cyprus, Nicosia, Cyprus
 - 31 University of Nymegen and NIKHEF, NL-6525 ED Nymegen, The Netherlands
 - 32 Oak Ridge National Laboratory, Oak Ridge, TN 37831, USA
 - 33 California Institute of Technology, Pasadena, CA 91125, USA
 - 34 INFN-Sezione di Perugia and Università Degli Studi di Perugia, I-06100 Perugia, Italy
 - 35 Carnegie Mellon University, Pittsburgh, PA 15213, USA
 - 36 Princeton University, Princeton, NJ 08544, USA
 - 37 INFN-Sezione di Roma and University of Rome, "La Sapienza", I-00185 Rome, Italy
 - 38 Nuclear Physics Institute, St. Petersburg, Russia
 - 39 University and INFN, Salerno, I-84100 Salerno, Italy
 - 40 University of California, San Diego, CA 92093, USA
 - 41 Dept. de Física de Partículas Elementales, Univ. de Santiago, E-15706 Santiago de Compostela, Spain
 - 42 Bulgarian Academy of Sciences, Central Laboratory of Mechatronics and Instrumentation, BU-1113 Sofia, Bulgaria
 - 43 Center for High Energy Physics, Korea Advanced Inst. of Sciences and Technology, 305-701 Taejon, Republic of Korea
 - 44 University of Alabama, Tuscaloosa, AL 35486, USA
 - 45 Utrecht University and NIKHEF, NL-3584 CB Utrecht, The Netherlands
 - 46 Purdue University, West Lafayette, IN 47907, USA
 - 47 Paul Scherrer Institut, PSI, CH-5232 Villigen, Switzerland
 - 48 DESY-Institut für Hochenergiephysik, D-15738 Zeuthen, FRG
 - 49 Eidgenössische Technische Hochschule, ETH Zürich, CH-8093 Zürich, Switzerland
 - 50 University of Hamburg, D-22761 Hamburg, FRG
 - 51 High Energy Physics Group, Taiwan, China
- § Supported by the German Bundesministerium für Bildung, Wissenschaft, Forschung und Technologie
‡ Supported by the Hungarian OTKA fund under contract numbers 2970 and T14459.
b Supported also by the Comisión Interministerial de Ciencia y Tecnología

‡ Also supported by CONICET and Universidad Nacional de La Plata, CC 67, 1900 La Plata, Argentina
◇ Also supported by Panjab University, Chandigarh-160014, India

Figure 1. Examples of possible diagrams responsible for the $B_{d,s}^0 \rightarrow \gamma\gamma$ decay. In these diagrams $q = u, c$ or t . H represents a possible charged Higgs particle.

Figure 2. Comparison of a) E_{Total} , the total energy of the two photons and b) $\theta_{\gamma\gamma}$, the opening angle between the two photons; for combinatorial background from data and five flavor $q\bar{q}$ Monte Carlo in contrast to exclusive $B^0 \rightarrow \gamma\gamma$ Monte Carlo events.

Figure 3. The measured $\gamma\gamma$ invariant mass distribution after all the selection cuts for the Monte Carlo a) $B_d^0 \rightarrow \gamma\gamma$ and b) $B_s^0 \rightarrow \gamma\gamma$ decays. The solid line is the result of a fit using a Gaussian function. The measured $\gamma\gamma$ invariant mass distribution for c) all events and d) the $b\bar{b}$ enriched sample, in data and Monte Carlo. The $b\bar{b}$ enriched sample is fitted with an exponential function excluding the $B_{d,s}^0$ mass window shown with dotted lines.

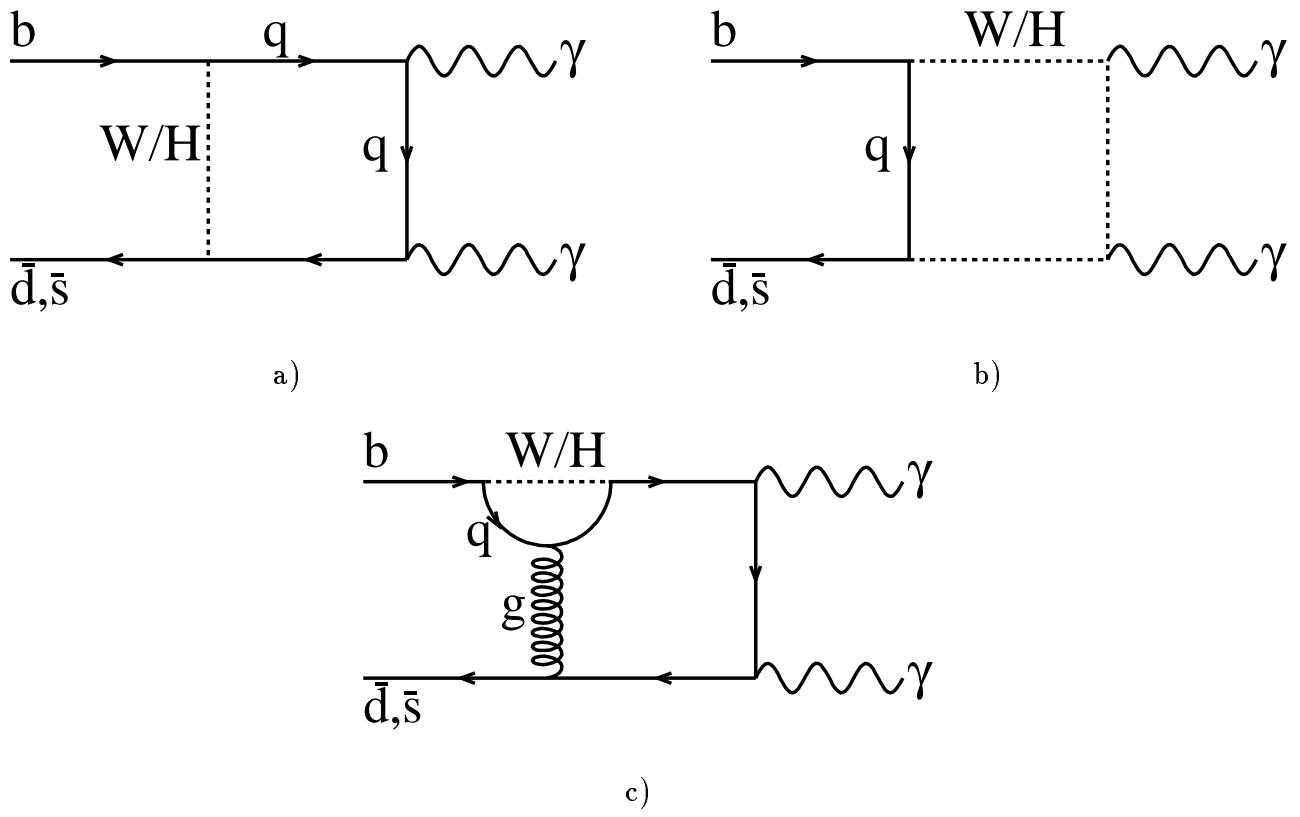


Figure 1

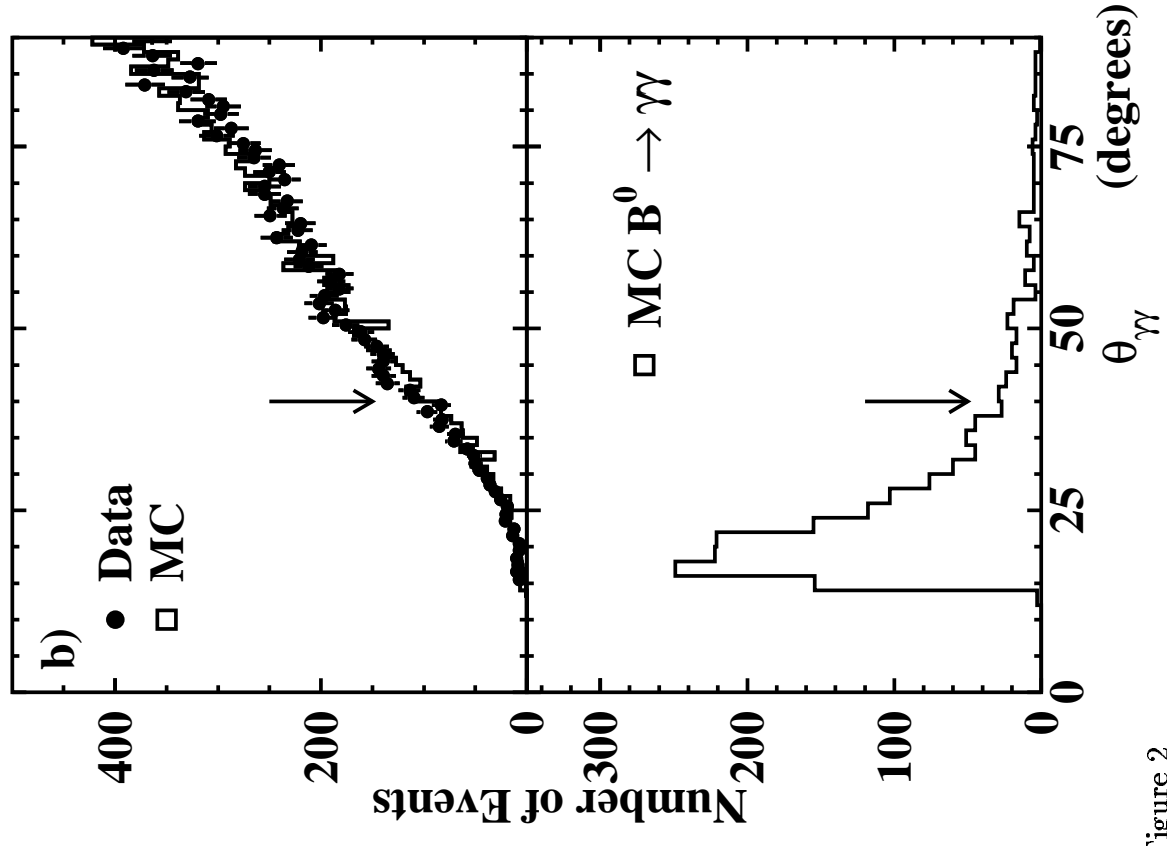
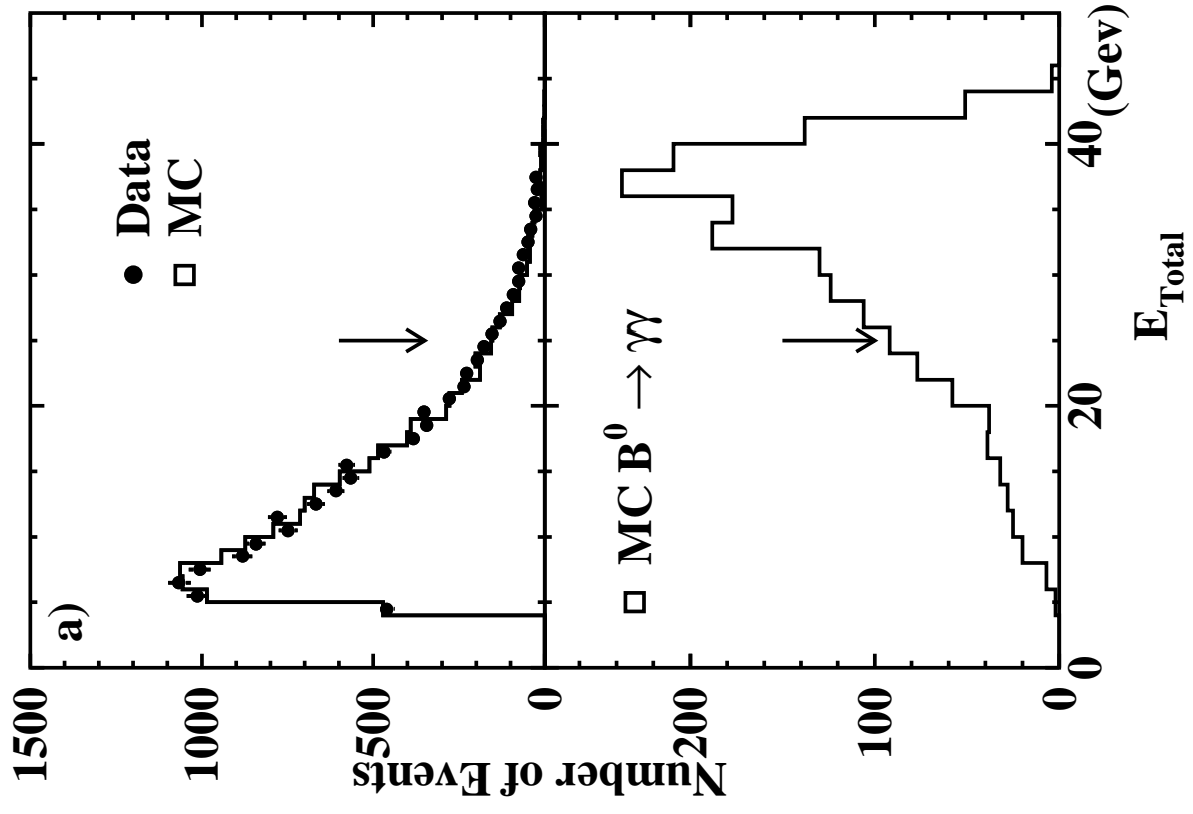


Figure 2

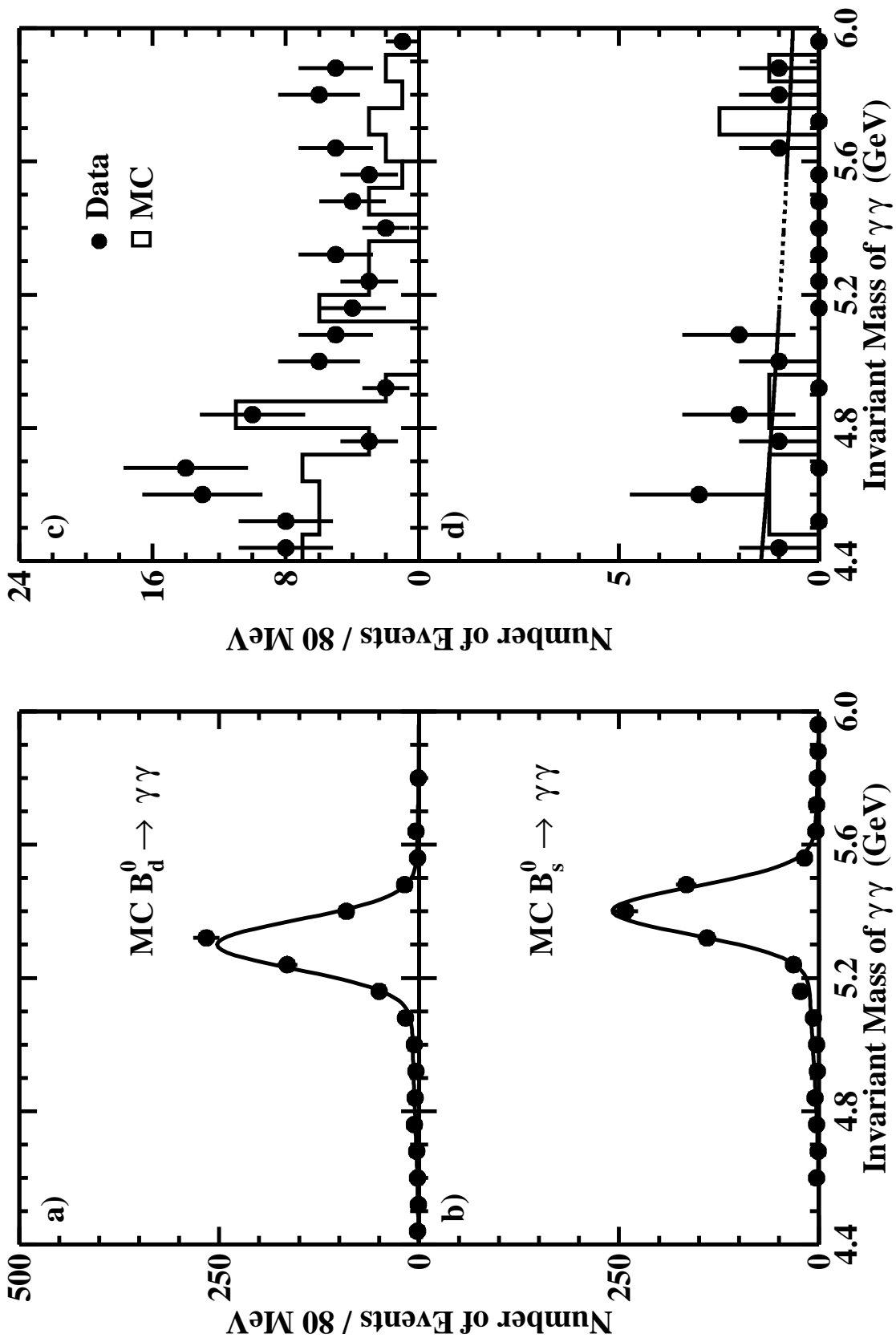


Figure 3